ResearchGate

See discussions, stats, and author profiles for this publication at: https://www.researchgate.net/publication/244653369

Specific features of the substitution of Fe 3+ impurity ions for Zr 4+ in NaZr 2 (PO 4) 3 single crystals

Article *in* Crystallography Reports · September 2005

DOI: 10.1134/1.2049404

CITATIONS
2

READS
34

9 authors, including:

Vladimir M Vinokurov
Kazan (Volga Region) Federal University
25 PUBLICATIONS **90** CITATIONS
SEE PROFILE

Akhmet Galeev
Kazan (Volga Region) Federal University
26 PUBLICATIONS **76** CITATIONS
SEE PROFILE

Nailia Khasanova
Kazan (Volga Region) Federal University
33 PUBLICATIONS **78** CITATIONS
SEE PROFILE

Sergey Stefanovsky
A. N. Frumkin Institute of Physical Chemistry a…
266 PUBLICATIONS **1,065** CITATIONS
SEE PROFILE

Some of the authors of this publication are also working on these related projects:

The Structure of Actinide-Bearing Glasses and Actinide Speciation View project

Pore size distribution in sedimentary rocks View project

All content following this page was uploaded by Akhmet Galeev on 29 July 2014.

The user has requested enhancement of the downloaded file.

Crystallography Reports, Vol. 50, No. 5, 2005, pp. 827–835. Translated from Kristallografiya, Vol. 50, No. 5, 2005, pp. 892–899.
Original Russian Text Copyright © 2005 by Bulka, Vinokurov, Galeev, Denisenko, Khasanova, Kanunnikov, Nizamutdinov, Stefanovsky, Trul.

PHYSICAL PROPERTIES OF CRYSTALS

Specific Features of the Substitution of Fe^{3+} Impurity Ions for Zr^{4+} in $NaZr_2(PO_4)_3$ Single Crystals

G. R. Bulka*, V. M. Vinokurov*, A. A. Galeev*, G. A. Denisenko, N. M. Khasanova*, G. V. Kanunnikov**, N. M. Nizamutdinov*, S. V. Stefanovsky***, and A. Yu. Trul*****

** Kazan State University, Kremlevskaya ul. 18, Kazan, 420008 Tatarstan, Russia*
e-mail: Vladimir.Vinokurov@ksu.ru
*** Shubnikov Institute of Crystallography, Russian Academy of Sciences, Leninskiĭ pr. 59, Moscow, 119333 Russia*
**** NPO Radon, Sed'moĭ Rostovskiĭ per. 2/14, Moscow, 119121 Russia*
Received December 20, 2004

Abstract—The EPR spectra of Fe^{3+} impurity ions in $NaZr_2(PO_4)_3$ single crystals at 300 K are investigated, and the spin Hamiltonian of these ions is determined. A comparative analysis of the spin-Hamiltonian and crystal-field tensors is performed using the maximum invariant component method. It is demonstrated that Fe^{3+} impurity ions substitute for Zr^{4+} ions with local compensator ions located in cavities of the *B* type. It is revealed that the invariant of the spin-Hamiltonian tensor B_4 and the crystal-field tensor V_4^{44} depend substantially on the mutual arrangement of ions in the first and second coordination spheres. The corresponding dependences are analyzed. © *2005 Pleiades Publishing, Inc.*

INTRODUCTION

Sodium zirconium phosphate $NaZr_2(PO_4)_3$ has a mixed framework $M_2(TO_4)_3$ [1] of the rhombohedral type [2]. This material is promising for use as an ionic conductor [3] and a ceramic matrix for immobilization of radioactive wastes for their long-term storage [4]. The $NaZr_2(PO_4)_3$ compound is the end member of the continuous series of $Na_{1+x}Zr_2Si_xP_{3-x}O_{12}$ (x = 0–3) solid solutions, in which the heterovalent substitution of impurity ions for host ions leads to a redistribution of filling cations in the structure [5] and to a change in the crystal field in the substitution region. Structural investigations by the EPR method allow one to elucidate the influence of impurity ions on the distribution of mobile ions in the structure.

When studying the crystals by the EPR method, the location of an impurity ion in the ground state with spin $S \geq 5/2$ in the case of nonlocal charge compensation can be reliably determined from the topological parameters of the spin-Hamiltonian tensor B_4 and the irreducible quadratic tensor product $\{V_4 \otimes V_4\}_4 = V_4^{44}$ of the crystal-field tensor V_4 [6, 7]. A comparative analysis of the spin-Hamiltonian and crystal-field tensors is performed using the point-charge model by ignoring the disturbance of the field in the substitution region of the central ion. The presence of a charge compensator in the substitution region substantially changes the spin-Hamiltonian tensor B_2. Hence, the location of the compensator ion, as a rule, is determined from a comparative analysis of the tensor B_2 and the second-rank irreducible quadratic tensor product $\{V_4 \otimes V_4\}_2 = V_2^{44}$ of the crystal-field tensor V_4 [6, 7].

In order to justify the correctness of these approximations as applied to point defects in the crystal, it is necessary to extend the classes of objects and to analyze objects belonging to different classes. For this purpose, dielectric crystals with ionic conductivity seem to be appropriate systems in which the locations of filling cations are governed by the framework structure and have been determined by diffraction methods.

The purpose of this work was to investigate in detail the angular dependence of the Fe^{3+} EPR spectra of $NaZr_2(PO_4)_3$ single crystals and to calculate and analyze their spin-Hamiltonian and crystal-field tensors comparatively.[1]

The spin-Hamiltonian and crystal-field irreducible tensors A_L of rank L are analyzed using the maximum invariant component (MIC) method [8], which is based on the examination of the part $S_L(G_S)$ of the invariant S_L

[1] The preliminary results were reported at the International Conference "Spectroscopy, X-ray Diffraction, and Crystal Chemistry of Minerals" (Kazan, 1997); the International Conference on Growth and Physics of Crystals, Dedicated to the Memory of M.P. Shaskolskaya (Moscow, 1998); the France–Spain Conference on Chemistry and Physics of Solids (Carcans–Buisson, 2000); and the 4th National Conference on Application of X-ray, Synchrotron, Neutron, and Electron Radiation to Investigation of Materials (Shubnikov Institute of Crystallography, Russian Academy of Sciences, Moscow, 2003).

1063-7745/05/5005-0827$26.00 © 2005 Pleiades Publishing, Inc.

of the tensor A_L in the unitary group U upon rotation of the coordinate system. It should be noted that $S_L(G_S)$ is the invariant of the subgroup G_S of the group U. Unlike the conventional use of the invariant combinations of the internal-field parameters for describing low-symmetry activator centers in crystals and glasses [9], the invariants used in the MIC method are applied to the determination of the spatial orientation of the tensors. In order to elucidate the role played by the invariants in analyzing the intrinsic and orientational properties of the tensors, in this paper, we discuss an analogue of the MIC method and the method of the transformation of the quadratic forms and equations of second-order surfaces into their canonical forms. We also consider the dependence of the invariants of the spin-Hamiltonian and crystal-field tensors on the mutual arrangement of the first and second coordination spheres of a paramagnetic ion.

THE CANONICAL FORM OF THE SPIN HAMILTONIAN

The location of an impurity paramagnetic ion in a single crystal is determined by analyzing the tensors B_L of the spin Hamiltonian $\hat{H}$ with the MIC and topological methods [10]. The spin Hamiltonian $\hat{H}$ can be written in the form

$$\hat{H} = \beta\hat{S}g\overline{H} + \sum_L \hat{H}_L,$$

where

$$\hat{H}_L = \sum_{M=-L}^{L} T_{LM}(\hat{S})A_{LM} = \sum_{M=-L}^{L} B_{LM}T_{LM}(\hat{S}) \quad (1)$$

and L = even number.

By using the second-rank tensor B_2 as an example, we will demonstrate that these methods, as applied to the EPR method, are similar to the methods used to investigate polynomials and hypersurfaces in analytic geometry [11].

Let $X_0Y_0Z_0$ be the Cartesian coordinate system in which the tensors of the spin Hamiltonian (1) are defined. The indicating surface of the tensor of rank $L = 2$ [7, 10] can be expressed through the Euler angles (α, β, $\gamma = 0$): $B_{20}(\alpha\beta) = \sqrt{3/2}\,(B_{22}\cos 2\alpha - B_{2-2}\sin 2\alpha)\sin^2\beta - \sqrt{6}\,(B_{21}\cos\alpha - B_{2-1}\sin\alpha)\sin\beta\cos\beta + (1/2)B_{20}(3\cos^2\beta - 1)$. By using the designations $x = \sin\beta\cos\alpha$, $y = \sin\beta\sin\alpha$, and $z = \cos\beta$, this surface is rearranged into the form $B_{20}(x, y, z) = a_{11}x^2 + a_{22}y^2 + a_{33}z^2 + 2a_{12}xy + 2a_{13}xz + 2a_{23}yz + a_{44}$, where $a_{11} = \sqrt{3/2}\,B_{22}$, $a_{22} = -\sqrt{3/2}\,B_{22}$, $a_{33} = (3/2)B_{20}$, $a_{44} = -B_{20}/2$, $a_{12} = -\sqrt{3/2}\,B_{2-2}$, $a_{13} = -\sqrt{3/2}\,B_{21}$, and $a_{23} = \sqrt{3/2}\,B_{2-1}$. The surface $B_{20}(x, y, z)$ is defined on a unit sphere $x^2 + y^2 + z^2 = 1$.

By rotating the $X_0Y_0Z_0$ coordinate system, it is possible to find the $X'Y'Z'$ coordinate system in which the indicating surface $B_{20}(x, y, z)$ has the canonical form [11]: $B_{20}(x', y', z') = a'_{11}x'^2 + a'_{22}y'^2 + a'_{33}z'^2 + a'_{44}$, where $a'_{11} = \sqrt{3/2}B'_{22}$, $a'_{22} = -\sqrt{3/2}B'_{22}$, $a'_{33} = 3/2\,B'_{20}$, and $a'_{44} = -1/2\,B'_{20}$. Depending on the sign of the ratio B'_{22}/B'_{20}, the function $B_{20}(x', y', z')$ can be represented in the following form: $B_{20}(x', y', z') = 1/2\,B'_{20}\,(\pm x'^2/a^2 \mp y'^2/a^2 + z'^2/c^2 - 1)$, where $1/a^2 = \sqrt{6}\eta$, $\eta = |B'_{22}/B'_{20}|$, and $1/c^2 = 3$. It can be seen that the indicating surface of the tensor B_2 has the external symmetry group $D_{2h} = 3L_2 3PC$ [12], whose twofold axes are parallel to the axes of the $X'Y'Z'$ coordinate system and are principal.

The topology of the indicating surface of the tensor B_2 is determined by the characteristic equation $B_{20}(x, y, z) = 0$, which, in the $X'Y'Z'$ coordinate system, has the form $B_{20}(x', y', z') = 0$ or $\pm x'^2/a^2 \mp y'^2/a^2 + z'^2/c^2 = 1$. This equation coincides with the canonical equation for a one-sheeted hyperboloid. The indicating and characteristic surfaces have identical symmetries and principal axes. The intersection of a one-sheeted hyperboloid with a sphere of radius $R = 1$ separates the sphere into three parts: one part differs from the other parts by the sign of $B_{20}(x', y', z')$.

At $\eta = 0$, the zeros of the function $B_{20}(x', y', z')$ are represented by the circles $x'^2 + y'^2 = 2/3$ at the height $z' = \pm\sqrt{1/3}$. At $B'_{22}/B'_{20} > 0$ and $0 < \eta \le 1/\sqrt{6}$, we have $a^2 \ge 1$ and a throat ellipse ($y' = 0$) intersects the unit sphere at the points $x'^2 = 2a^2/(3a^2 - 1)$ and $z'^2 = (a^2 - 1)/(3a^2 - 1)$. In this case, the lines of the zero level are symmetrically located with respect to the plane $z' = 0$. At $\eta > 1/\sqrt{6}$, we have $a^2 < 1$ and the throat ellipse does not intersect the unit sphere; i.e., the intersection lines of the sphere and the hyperboloid are located on different sides of the plane $y' = 0$.

In order to determine the system of the principal axes of the tensor B_2 by the MIC method, the invariant $S_2 = (B_{20})^2 + 2\sum_{M=1}^{2}[(B_{2M})^2 + (B_{2-M})^2]$ in any coordinate system XYZ obtained through rotation of the coordinate system $X_0Y_0Z_0$ is represented as the sum $S_2 = S_2(D_{2h}) + S_{2r}$, where $S_2(D_{2h}) = (B_{20})^2 + 2(B_{22})^2$. The XYZ axes coincide with the $3L_2$ axes of the group D_{2h}. The coordinate system in which the quantity $S_2(D_{2h})$ takes the maximum value, $\max S_2(D_{2h}) = S_2 = (B'_{20})^2 + 2(B'_{22})^2$, represents the system of the principal axes. The system of the principal axes can also be determined by diagonalizing the corresponding second-rank Cartesian tensor.

However, there exist a number of problems that can be solved only using the MIC method. Let us determine the measure of deviation of the tensor B_2 from symmetry $D_{\infty h}$. When the tensor B_2 has symmetry $D_{\infty h}$, the Z'

axis of the $X'Y'Z'$ coordinate system in which $S_2 = (B_{20})^2$ is the axis ∞ of the group $D_{\infty h}$. If the symmetry is distorted with respect to the symmetry group $D_{\infty h}$, the invariant S_2 in the XYZ coordinate system is represented as the sum $S_2 = S_2(D_{\infty h}) + S_{2r}$, where $S_2(D_{\infty h}) = (B_{20})^2$. By rotating the XYZ coordinate system, we find the coordinate system (XYZ, $D_{\infty h}$) in which the term $S_2(D_{\infty h})$ takes the maximum value, $\max S_2(D_{\infty h})$. The quantity $d = [S_2 - \max S_2(D_{\infty h})]/S_2$ is the measure of deviation of the tensor B_2 from symmetry $D_{\infty h}$.

The MIC method appears to be indispensable in a comparative analysis of tensors B_L of rank $L \geq 4$ that are irreducible with respect to the group of continuous rotations. The characteristic equation $B_{L0}(\alpha, \beta) = 0$ at $L \geq 4$ that determines the zero level of the indicating surface corresponds to a more complex topology [7].

SAMPLE PREPARATION AND EXPERIMENTAL TECHNIQUE

Single crystals of $NaZr_2(PO_4)_3$ were grown by the solution–melt method with the use of the initial reagents Na_2CO_3, ZrO_2, $NH_4H_2PO_4$, NaF, and V_2O_5 taken in the ratio (mol %) $0.07Na_2O : 0.07ZrO_2 : 0.32P_2O_5 : 0.47NaF : 0.07V_2O_5$ [13]. Crystallization was performed by cooling the system at a rate of 0.5 K/h in the temperature range 950–800°C. After completing the process, the platinum bar was removed from the solution and cooled to room temperature at a rate of 50 K/h. The crystals grown had the form of individual rhombohedra. Moreover, the single crystals were grown with the use of the initial batch containing MoO_2.

The EPR spectra were recorded at a frequency ν = 9.4 GHz and a temperature of 300 K on a DX 70-02 EPR spectrometer (SKB Analitpribor, Belarussian State University, Minsk). The sensitivity of the spectrometer to impurities was equal to 10^{14} spins/G. In order to investigate the spectra of the single-crystal samples in detail, the spectrometer was equipped with a specially designed goniometer. The high-quality spectra were obtained by their prolonged accumulation.

ELECTRON PARAMAGNETIC RESONANCE OF Fe^{3+} IONS IN A $NaZr_2(PO_4)_3$ SINGLE CRYSTAL

The EPR study was performed using isometric crystals ~2 mm in size with rhombohedral faces of the $[11\bar{2}4]$ type. The samples grown from the melt containing the molybdenum dopant are characterized by the narrowest and most intense lines (Fig. 1). The EPR spectra involve lines of Cr^{3+}, Mn^{2+} (~10^{-5} wt %), and Fe^{3+} (~$n \times 10^{-4}$ wt %) impurities. In the present work, we thoroughly examined only the Fe^{3+} EPR spectra. The preliminary investigation into the angular dependence of the EPR spectra revealed that, at $H \parallel [0001]$, six symmetry-related Fe^{3+} EPR spectra (K_M = 6) are merged together (Fig. 1a). According to the space group $D_{3d}^6 - R\bar{3}c$ of the $NaZr_2(PO_4)_3$ structure [1], the multiplicity K_M = 6 corresponds to the position with the Laue symmetry group C_i. On this basis, the spin Hamiltonian (1) with symmetry C_i was chosen for describing one symmetry-related spectrum.

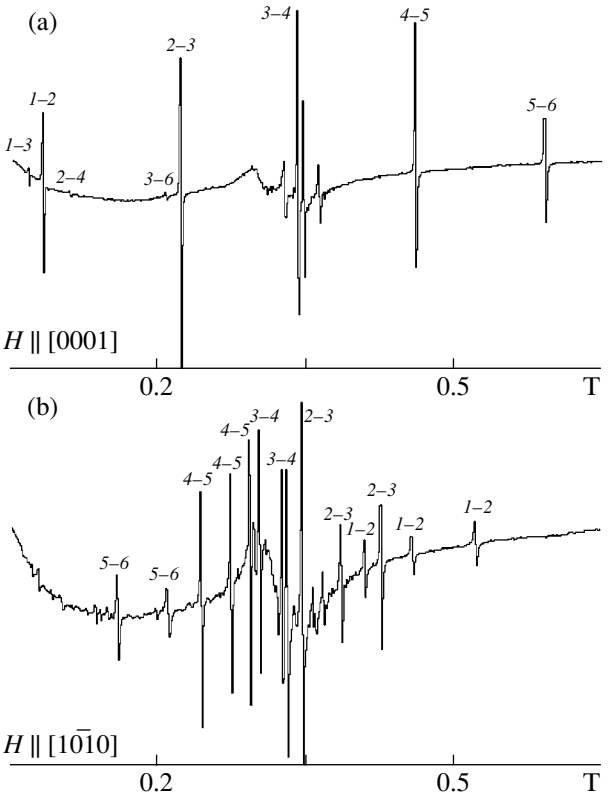

Fig. 1. Fe^{3+} EPR spectra of $NaZr_2(PO_4)_3$ crystals at a frequency ν = 9.4 GHz and at a temperature of 300 K in magnetic fields (a) $H \parallel [0001]$ and (b) $H \parallel [10\bar{1}0]$. The identification of the transitions corresponds to the energy-level diagram in Fig. 3.

The direction of the field **H** in the spin Hamiltonian (1) is described by the unit vector $\mathbf{n}[\sin\theta\cos\varphi, \sin\theta\sin\varphi, \cos\theta]$ in the coordinate system with the axes $X_0 \parallel L_2$, $Y_0 \parallel P$, and $Z_0 \parallel L_3$. The L_2 and L_3 axes and the P plane are the symmetry elements in the group D_{3d} of the crystal. The coordinate systems for each six symmetry-related positions of Fe^{3+} ions are related by the symmetry elements of the group $D_3 \subset D_{3d}$, which are represented by the Euler angles (α, β, γ): $E \longleftrightarrow (0, 0, 0)$, $3_1 \longleftrightarrow (2\pi/3, 0, 0)$, $3_2 \longleftrightarrow (-2\pi/3, 0, 0)$ $2_x \longleftrightarrow (0, \pi, \pi)$, $2_{xy} \longleftrightarrow (0, \pi, \pi/3)$, and $2_{\bar{x}y} \longleftrightarrow (-\pi/3, \pi, 0)$. In these local coordinate systems, the unit vector **n** has the coordinates $[\sin\theta\cos\varphi, \sin\theta\sin\varphi, \cos\theta]$, $[-\sin\theta\cos(\varphi + 60), -\sin\theta\sin(\varphi + 60), \cos\theta]$, $[-\sin\theta\cos(\varphi - 60), -\sin\theta\sin(\varphi - 60), \cos\theta]$, $[\sin\theta\cos\varphi, -\sin\theta\sin\varphi, -\cos\theta]$, $[-\sin\theta\cos(\varphi + 60), \sin\theta\sin(\varphi + 60), -\cos\theta]$,

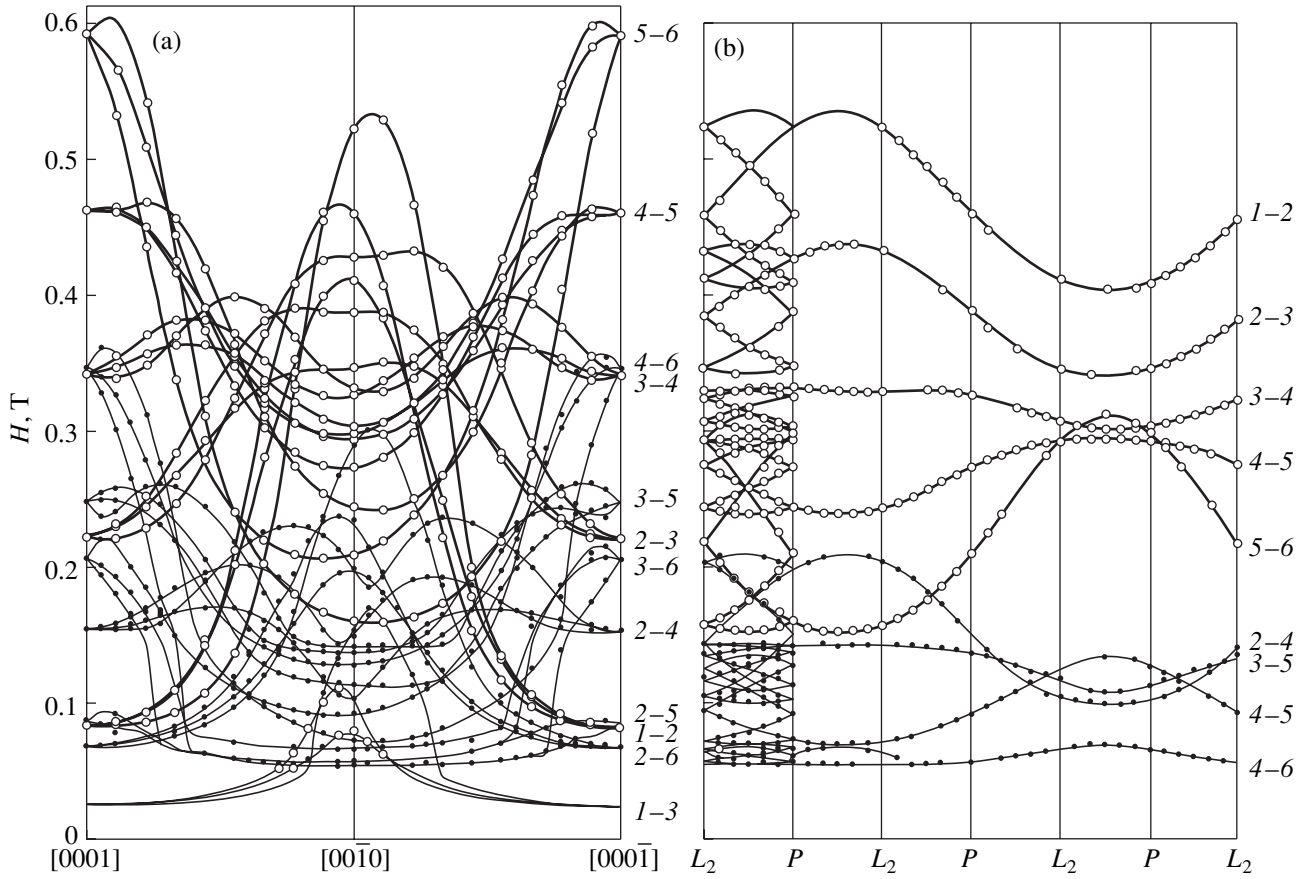

Fig. 2. Angular dependences of the Fe^{3+} EPR spectrum for the $NaZr_2(PO_4)_3$ crystal in the (a) (1210) and (b) (0001) crystallogarphic planes. Open and closed circles indicate the measured resonance fields H for the transitions at $\Delta M = 1$ and $\Delta M \neq 1$, respectively. Lines represent the resonance fields H calculated from the spin-Hamiltonian parameters. The identification of the transitions corresponds to the energy-level diagram in Fig. 3.

and $[-\sin\theta\cos(\varphi - 60), \sin\theta\sin(\varphi - 60), -\cos\theta]$, respectively.

In order to choose the planes for detailed measurements of the spectra, we analyzed the dependences of the tensors B_2 and B_4 of the spin Hamiltonian (1) on the Euler angles ($\alpha = \varphi$, $\beta = \theta$, $\gamma = 0$) [7] within the exact independent domain of the group D_{3d} [14]. In this domain, we restricted ourselves to two forms represented by the dihedral angle between the $(01\bar{1}0)$ and $(\bar{1}2\bar{1}0)$ planes [14] and the trihedral angle with the $(\bar{1}2\bar{1}0)$, $(\bar{2}110)$, and (0001) faces [15]. The boundaries of these forms can be set and controlled using the arrangement of the symmetry-related EPR spectra. When the Zeeman energy is comparable or larger than the initial splittings, the angular dependence of the EPR spectrum is predominantly governed by the diagonal elements $B_{20}(\varphi, \theta)$ and $B_{40}(\varphi, \theta)$ of the spin Hamiltonian, i.e., by indicating surfaces of the tensors. Consequently, with the aim of increasing the accuracy of the determination of the spin-Hamiltonian parameters, the planes for measurements of the spectra within the exact independent domain should be chosen so that all the tensor elements contribute to the dependences $B_{20}(\varphi, \theta)$ and $B_{40}(\varphi, \theta)$. In EPR studies, when the spin-Hamiltonian matrix is numerically diagonalized, the planes for measurements are chosen taking into account the requirements for the minimization of the time of spectrum recording. In our experiments, the angular dependences were measured in the $(\bar{1}2\bar{1}0)$ and (0001) planes (Figs. 2a, 2b). The angular dependence of three doubly degenerate symmetry-related EPR spectra in the $(\bar{1}2\bar{1}0)$ plane (Fig. 2a) permits us to determine reliably all the spin-Hamiltonian parameters, except the element B_{43}.

In order to determine the element B_{43}, we measured the angular dependence of all six symmetry-related EPR spectra in the (0001) plane at $0° \le \varphi \le 30°$ (Fig. 2). These data make it possible to construct the dependence of any symmetry-related EPR spectrum in the range $0° \le \varphi \le 180°$ in the (0001) plane.

By using the components of the vector **H** in the local coordinate systems, the spin-Hamiltonian parameters (table) were calculated according to a program similar to that described in [16]. The dependence of the energy

levels and their differences on the external magnetic field **H** is shown in Fig. 3.

ANALYSIS OF THE SPIN-HAMILTONIAN AND CRYSTAL-FIELD TENSORS

The structure of the $NaZr_2(PO_4)_3$ crystal [1] was analyzed in order to determine the location of Fe^{3+} impurity ions in this crystal. The $NaZr_2(PO_4)_3$ framework has the space group $R\bar{3}c - D_{3d}^6$ and can be represented as a rhombohedral unit cell whose vertices and center are occupied by lanterns. The structure of the central lantern turns out to be inverted with respect to the structure of the lanterns located at the vertices, and this lantern serves as a bridge between the latter lanterns [2]. The M_2T_3 lantern is composed of two *M* octahedra [ZrO_6] with a common triple axis and three *T* tetrahedra [PO_4] (Fig. 4). The parallel edges of this linking tetrahedra form an empty trigonal prism with symmetry D_3 between octahedra. In this framework, the M_2T_3 lanterns alternate along the triple axis and form octahedral cavities of the *A* type. Between columns, there are *B*-type cavities formed by ten O^{2-} ions (Fig. 4).

In the $NaZr_2(PO_4)_3$ structure, the ions of the framework occupy the following positions with the symmetry groups G_α: Zr^{4+}, 12*c* ($G_\alpha = C_3$); P^{5+}, 18*e* ($G_\alpha = C_2$); O_I, 36*f* ($G_\alpha = C_1$); and O_{II}, 36*f* ($G_\alpha = C_1$). The Na^+ ions compensate for the framework charge, fill all cavities of the *A* type, and occupy the 6*b* positions ($G_\alpha = C_{3i}$). The *B* cavities correspond to the 18*e* positions ($G_\alpha = C_2$) and alternate with the P^{5+} ions.

We can assume that Fe^{3+} impurity ions in the $NaZr_2(PO_4)_3$ structure occupy the Zr^{4+} positions arranged similarly to the Fe^{3+} ions in the $Na_3Fe_2(PO_4)_3$ structure [3]. In the $NaZr_2(PO_4)_3$ structure (Fig. 4), there are two magnetically related Zr^{4+} positions with the coordinates ($x = 0$, $y = 0$, $z = 0.64568$) and ($x = 0$, $y = 0$, $z = 0.85432$). In order to assign the spin-Hamiltonian tensor to one of these positions, the crystal-field tensor V_4^{44} was calculated using the point-charge model for the [ZrO_6] octahedron. In the coordinate system ($X_0 \parallel L_2$, $Y_0 \parallel P$, $Z_0 \parallel L_3$), the ξ, η, and ζ principal axes of the cubic components of the fourth-rank spin-Hamiltonian tensor B_4 and the fourth-rank crystal-field tensor V_4^{44} for the Zr^{4+} position with the coordinates ($x = 0$, $y = 0$, $z = 0.64568$) are determined by the following matrices of the direction angles.

B_4	X_0	Y_0	Z_0
ξ	118.68	47.3	123.82
η	143.44	94.85	53.87
ζ	69.34	43.11	54.18

V_4^{44}	X_0	Y_0	Z_0
ξ	117.91	48.01	125.26
η	144.43	94.06	54.74
ζ	69.80	42.28	54.74

(2)

Good agreement between the direction angles of the ξ, η, and ζ principal axes (the differences do not exceed 1.5°) for these tensors and the insignificant deviation from cubic symmetry $d_4(B_4, O_h) = 0.57 \times 10^{-2}$, $d_4(V_4^{44}, O_h) = 0.38 \times 10^{-2}$ confirm that Fe^{3+} ions occupy the Zr^{4+} positions in the $NaZr_2(PO_4)_3$ structure. The existence of six symmetry-related spectra is associated with the fact that the compensator ion is not located on the triple axis of the substituted position. The mobility of the Na^+ compensator ion suggests that similar ions are located in the *B* cavities in the structure. The coordinates of the compensator ions in the *B* cavities were refined by minimizing the sum of the squares of the deviations of the corresponding elements of the normalized crystal-field tensor V_2^{44} from the elements of the spin-Hamiltonian tensor B_2: $\sigma^2 = \sum_{M=-L}^{L}[B_{LM} - V_{LM}^{44}(S_L(B_L)/S_L(V_L^{44}))^{1/2}]^2$. The crystal-field elements were calculated with due regard for the contribution from the ions in the coordination sphere 35 Å in radius. The elements of the spin-Hamiltonian tensor correspond to the compensator ion with the coordinates ($x = -0.3062$, $y = -0.2336$, $z = 0.7319$) in the *B* cavity with the center ($x = -0.30736$, $y = -0.30736$, $z = 3/4$). In this case, the discrepancy factor was determined to be $\sigma^2/S_2(B_2) = 0.01$ and the matrices of the direction angles of the *X*, *Y*, and *Z* principal axes of the spin-Hamiltonian tensor B_2 and the crystal-field tensor V_2^{44} are in reasonable agreement:

B_2	X_0	Y_0	Z_0
X'	44.03	134.0	90.33
Y'	46.28	44.44	83.54
Z'	94.25	94.87	6.47

V_2^{44}	X_0	Y_0	Z_0
X'	44.95	134.44	95.44
Y'	45.07	45.79	82.98
Z'	91.12	98.82	8.89

The local compensator ion only weakly disturbs the crystal field at the Zr^{4+} position. In order to confirm this assumption, we calculated the direction angles of the L_3 principal axes of the maximum invariant components with symmetry $G_S = C_3$ ($\alpha, \beta, \gamma = 0$) and the parameters d_4 characterizing the deviation from symmetry C_3 of the spin-Hamiltonian tensor B_4 and the crystal-field tensor V_4^{44}. The results of calculations are presented in the following tables:

B_4	α, deg	β, deg	γ, deg	$d_4 \times 10^{-2}$
L_3	124.87	68.94	0	0.48
L_3	135.46	1.56	0	0.03
L_3	65.49	108.97	0	0.52
L_3	184.56	108.48	0	0.54

V_4^{44}	α, deg	β, deg	γ, deg	$d_4 \times 10^{-2}$
L_3	125.22	70.67	0	0.30
L_3	145.68	0.15	0	0.01
L_3	65.15	109.53	0	0.25
L_3	185.23	109.61	0	0.27

It can be seen from these data that the L_3 principal axes of the maximum invariant components with symmetry $G_S = C_3$ for the spin-Hamiltonian tensor B_4 and the crystal-field tensor V_4^{44} only slightly deviate from the [0001] axis in the crystal and are characterized by insignificant deviation from symmetry C_3.

DISCUSSION OF THE RESULTS AND CONCLUSIONS

Analysis of the spin-Hamiltonian and the crystal-field tensors conclusively demonstrates that Fe^{3+} impurity ions substitute for Zr^{4+} ions with local charge compensation and lowering of position symmetry. The Na^+ compensator ions are located in cavities of the *B* type and weakly disturb the crystal field in the substitution region. Since Fe^{3+} impurity ions are randomly distributed in the structure, we can make the inference that compensator ions are mobile under the crystal-growth conditions. The fact that Fe^{3+} impurity ions occupy positions of one regular system of points indicates the absence of a statistical distribution of Na^+ ions in *B* cavities at a low concentration of Fe^{3+} ions. The multiplicity $K_M = 6$ and the arrangement of symmetry-related Fe^{3+} EPR spectra correspond to the space group $D_{3d}^6 - R\bar{3}c$ of the $NaZr_2(PO_4)_3$ crystal and confirm that $Na_{1+x}Fe_xZr_{2-x}(PO_4)_3$ solid solutions at low concentrations x have a structure similar to the $NaZr_2(PO_4)_3$ structure [18].

According to the intersection of the groups $C_3 \cap C_2 = C_1$ of the Zr^{4+} positions and *B* cavities, the substitution region $Fe^{3+} + Na^+ \longrightarrow Zr^{4+}$ has symmetry C_1. Therefore, it can be expected that the Na^+ compensator ion should be displaced from the symmetry axis and the *B* cavity center (determined as the center of gravity of the ten O^{2-} ions forming the cavity). This displacement

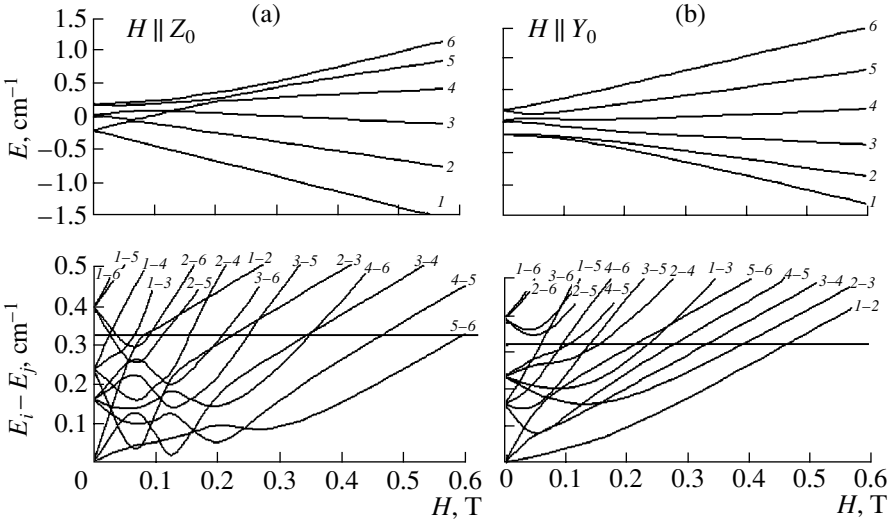

Fig. 3. Energy levels E_i and their differences ($E_i - E_j$) as functions of the magnetic field for the $NaZr_2(PO_4)_3$ crystal: (a) $H \parallel Z_0$ and (b) $H \parallel Y_0$. The line corresponds to the operating frequency ν = 9.4 GHz.

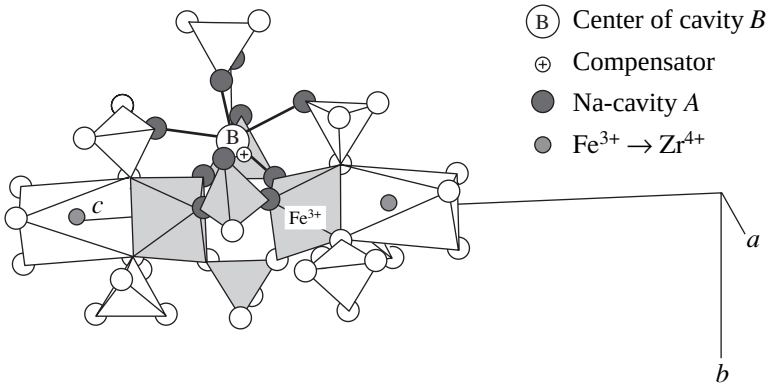

Fig. 4. Positions of the ions forming the crystal framework and the cavities in the $NaZr_2(PO_4)_3$ structure. Shaded octahedra and tetrahedra make up an M_2T_3 lantern. Closed circles indicate the O^{2-} ions forming the cavity *B*.

is 0.77 Å in the direction of the Fe^{3+} impurity ion. The displacement direction forms an angle of 10.3° with the vector connecting the *B* cavity center and the Zr^{4+} position (Fig. 4).

The distance between the Na^+ compensator ion and the Fe^{3+} impurity ion (3.13 Å) is considerably smaller than the distance from the Zr^{4+} position to the *B* cavity center (3.60 Å). This finding is in agreement with the fact that the distances between the dopant and Na^+ ions in the $Na_3Zr_{0.5}Co_{0.5}FeP_3O_{12}$ and $Na_3Zr_{0.5}Fe(II)_{0.5}Fe(III)P_3O_{12}$ compounds are shorter than the Zr^{4+}–Na^+ distance in the $NaZr_2(PO_4)_3$ crystal [19].

However, the distance between the Na^+ compensator ion and the nearest vertex of the $[ZrO_6]$ octahedron (1.85 Å) differs substantially from the sum of the Na^+ and Zr^{4+} radii (2.34 Å). Such a shortened distance is most likely associated with disregarding the displacement of other ions in the substitution region.

As follows from the direction angle matrices (2), the coordination polyhedron of the impurity ion can be determined using the model of point charges corresponding to the first coordination sphere. However, a comparative analysis of the invariant sums of the B_4 and V_4^{44} tensors for different structures, as well as of the systems of principal axes and the ratios of the principal components of the B_2 and V_4^{44} tensors, requires the inclusion of the contributions from more distant charges and the compensator ion. In $ZnSeO_4 \cdot H_2O$ crystals, the inclusion of the contribution from hydrogen ions of the $[Zn(H_2O)_6]$ octahedron to the tensor V_4 leads to satisfactory agreement of the aforementioned topological characteristics of the Mn^{2+} spin-Hamiltonian tensor B_2 and the crystal-field tensor V_2^{44} [6]. The heterovalent substitution $Fe^{3+} \longrightarrow Ge^{4+}$ in $Li_2Ge_7O_{15}$ crystals [7] is accompanied by the local compensation $OH^- \longrightarrow O^{2-}$, and good agreement between the systems of the principal axes of the tensors B_2 and V_2^{44} can be achieved only when the contribution of H^+ compensator ions is taken into account. By generalizing these data, we can argue that the point-charge model for the crystal field adequately describes the main orientational properties of the crystal structure and the spin-Hamiltonian tensors B_2 and B_4 depend quadratically on the crystal-field tensor V_4. At the same time, the tensor B_2 depends linearly on the noncubic elements of the tensor V_4.

Parameters B_{LM} of spin Hamiltonian (1), initial splittings Δ_i ($\times 10^4$ cm^{-1}) of the ground state of Fe^{3+} ions, and quantities S_L ($\times 10^8$ cm^{-2}) in the coordinate system ($X_0 \| L_2$, $Y_0 \| P$, $Z_0 \| L_3$) for the $NaZr_2(PO_4)_3$ single crystal

M, q	B_{2M}	b_2^q	B_{4M}	b_4^q
0	−486.597	−595.957	−4.025	−14.432
1	−55.055	330.330	0.204	−6.543
−1	60.834	365.004	0.227	7.280
2	−3.547	−10.641	0.163	3.696
−2	−118.682	356.046	−0.188	4.263
3			5.571	−472.715
−3			−1.487	−126.176
4			−0.174	−5.220
−4			−0.155	4.650

Δ_1 = 2336.5	S_2 = 278423.7	ε* = 7.7 (mT)	
Δ_2 = 1581.7	S_4 = 83.02	N = 139	k = 20

g tensor $g_{ij} = g_{ji}$

2.00593	0.00102	−0.00034
	2.00539	−0.00019
		2.00512

* $\varepsilon = \sqrt{\sum_{i=1}^{N} \Delta H_i^2/(N-k)}$ is the root-mean-square deviation, and b_2^q stands for the Stevens notation [17].

The invariant S_4 of the spin-Hamiltonian tensor B_4 for Fe^{3+} ions in the $NaZr_2(PO_4)_3$ crystal (table) appears to be unexpectedly close to values characteristic of the tetrahedral environment [7]. Such a small difference cannot be explained only by the Zr–O distances (2.0472, 2.0681 Å) in the $[ZrO_6]$ octahedron in the $NaZr_2(PO_4)_3$ structure. In the $CaCO_3$ calcite, an $[CaO_6]$ octahedron with a Ca–O distance of 2.3598 Å is characterized by the invariant $S_4 = 325 \times 10^{-8}$ cm^{-2} [8]. An increase in the value of S_4 with an increase in the *Me*–O distance is inconsistent with the concept regarding the decrease in the crystal field with an increase in the distance from a field source. A similar contradiction is observed when the invariant $S_4 = 369 \times 10^{-8}$ cm^{-2} [20] for $[TiO_6]$ octahedra characterized by the mean distance $\langle$Ti–O$\rangle$ = 1.977 Å in $KTiOPO_4$ crystals is compared with the invariant $S_4 = 448 \times 10^{-8}$ cm^{-2} [8] for Fe^{3+} ions in $[MgO_6]$ octahedra having the distance Mg–O = 2.0839 Å in the $CaMg(CO_3)_2$ dolomite structure. In order to resolve this contradiction, we examined the mutual arrangement of anion and cation coordination polyhedra with respect to central ions.

The maximum invariant $S_4 = 4735 \times 10^{-8}$ cm^{-2} [21] is observed upon substitution of Fe^{3+} ions for Al^{3+} ions in $[AlO_6]$ octahedra with the mean distance $\langle$Al–O$\rangle$ = 1.9109 Å in $YAlO_3$ crystals having the perovskite-type structure. In these crystals, O^{2-} and Y^{3+} ions comprise the three-layer closest packing; form octahedral and cubic environments of the substitution position, respectively; and make contributions of the same sign to the tensor V_4. The octahedral anion and cubic cation environments are dual. In $Y_3Al_5O_{12}$ garnet, the spin Hamiltonian of Fe^{3+} ions substituting for Al^{3+} ions in $[AlO_6]$ octahedra with an Al–O distance of 1.937 Å is characterized by the invariant $S_4 = 1266 \times 10^{-8}$ cm^{-2}. The substitution octahedron appears to be inside the strongly contracted and substantially elongated octahedra, whose vertices are occupied by Al^{3+} and Y^{3+} ions, respectively. Such an arrangement of cations and anions around the substitution position leads to a decrease in the invariant S_4 as compared to that for $YAlO_3$ crystals. In the $NaZr_2(PO_4)_3$ crystal, the second coordination sphere is formed by the octahedron composed of P^{5+} pentavalent ions. This results in a considerable weakening of the crystal field at the substitution position.

In the $KTiOPO_4$ structure, four vertices of the $[TiO_6]$ octahedron are represented by vertices of four $[PO_4]$ tetrahedra and the other vertices are occupied by "free" O^{2-} ions. In the $NaZr_2(PO_4)_3$ structure, the vertices of the $[ZrO_6]$ octahedron are formed by vertices of six $[PO_4]$ tetrahedra. The calculation of the crystal field with allowance made for the contribution from all the surrounding tetrahedra leads to the ratio $S_4(V_4^{44}, KTiOPO_4)/S_4(V_4^{44}, NaZr_2(PO_4)_3) = 4.6$, which virtually coincides with the ratio between the invariant sums $S_4(KTiOPO_4)/S_4(NaZr_2(PO_4)_3) = 4.4$ for the spin-Hamiltonian tensors B_4. For the $YAlO_3$ and $Y_3Al_5O_{12}$ compounds, similar calculations result in the ratio $S_4(V_4^{44}, YAlO_3)/S_4(V_4^{44}, Y_3Al_5O_{12}) = 4.4$, which is close to the experimental ratio $S_4(YAlO_3)/S_4(Y_3Al_5O_{12}) = 3.7$.

The point charges identical in sign at the vertices of a regular cube and a dual octahedron make the contributions opposite in sign to the tensor V_4. When the charges at the vertices of the cube differ in sign from those of the octahedron, the contributions from the fields of these environments to the tensor V_4 coincide in sign. It is known [22] that, in BaF_2 crystals, an F^- compensator ion located on the triple axis of the $[GdF_8]$ cube with an impurity ion $Gd^{3+} \longrightarrow Ba^{2+}$ leads to an increase in the invariant S_4 of the Gd^{3+} spin-Hamiltonian tensor as compared to a similar invariant without local charge compensation. In CaF_2 crystals, the F^- compensator ion in an $[GdF_8]$ cube neighboring along the quadruple axis results in a considerable decrease in the invariant S_4. A comparison of the above data makes it possible to draw the conclusion that the invariant sum S_4 is governed not only by the effective charges and *Me*–O distances in the first coordination sphere but also by the mutual arrangement of the first and second coordination spheres.

ACKNOWLEDGMENTS

This work was supported by the Ministry of Education of the Russian Federation, project no. E02-9.0-86.

REFERENCES

1. H. Hong, Mater. Res. Bull. **11**, 173 (1976).
2. V. V. Ilyukhin, A. A. Voronkov, and V. K. Trunov, Koord. Khim. **7**, 1603 (1981).
3. A. K. Ivanov-Shits and I. V. Murin, *Solid State Ionics* (S.-Peterb. Gos. Univ., St. Petersburg, 2000) [in Russian].
4. B. E. Sheetz, D. K. Agrawal, E. Brewal, and R. Roy, Waste Manage. Res. **14**, 15 (1994).
5. V. A. Efremov and V. B. Kalinin, Kristallografiya **23** (4), 703 (1978) [Sov. Phys. Crystallogr. **23** (4), 393 (1978)].
6. V. M. Vinokurov, A. R. Al-Soufi, A. A. Galeev, *et al.*, Appl. Magn. Reson. **7**, 323 (1994).
7. A. A. Galeev, N. M. Khasanova, A. V. Bykov, *et al.*, Appl. Magn. Reson. **11**, 61 (1996).
8. N. M. Khasanova, N. M. Nizamutdinov, V. M. Vinokurov, and G. R. Bulka, Kristallografiya **33** (5), 891 (1988) [Sov. Phys. Crystallogr. **33** (5), 527 (1988)].
9. A. K. Przhevuskiĭ, Opt. Spektrosk. **53** (4), 697 (1982) [Opt. Spectrosc. **53** (4), 414 (1982)]; Opt. Spektrosk. **53** (5), 837 (1982) [Opt. Spectrosc. **53** (5), 499 (1982)].

10. N. M. Nizamutdinov, N. M. Khasanova, A. A. Galeev, *et al.*, Kristallografiya **34** (4), 893 (1989) [Sov. Phys. Crystallogr. **34** (4), 536 (1989)].
11. V. A. Il'in and É. G. Poznyak, *Analytic Geometry* (Nauka, Moscow, 1981) [in Russian].
12. Yu. I. Sirotin and M. P. Shaskolskaya, *Fundamentals of Crystal Physics* (Nauka, Moscow, 1979; Mir, Moscow, 1982) [in Russian].
13. A. B. Bykov, L. N. Dem'yanets, S. N. Doronin, *et al.*, Rost Kristallov **16**, 44 (1986).
14. R. V. Galiulin, Kristallografiya **23** (6), 1125 (1978) [Sov. Phys. Crystallogr. **23** (6), 635 (1978)].
15. R. V. Galiulin, *Lectures on Geometrical Foundations of Crystallography* (Chelyabinsk Gos. Univ., Chelyabinsk, 1989) [in Russian].
16. G. Bacquet, J. Dugas, C. Escribe, *et al.*, J. Phys. C: Solid State Phys. **7**, 1551 (1974).
17. C. Rudowicz, Magn. Reson. Rev. **13**, 1 (1987); **13**, 335 (1988).
18. Takashi Asai, Kazuaki Ado, Yuria Saito, *et al.*, Solid State Ionics **35** (3–4), 319 (1989).
19. Hiroyuki Kageyama, Nagao Kamijo, Takashi Asai, *et al.*, Solid State Ionics **40–41** (1), 350 (1990).
20. N. M. Nizamutdinov, N. M. Khasanova, G. R. Bulka, *et al.*, Kristallografiya **32** (3), 695 (1987) [Sov. Phys. Crystallogr. **32** (3), 408 (1987)].
21. V. A. Akkerman, G. R. Bulka, D. I. Vaĭnshteĭn, *et al.*, Fiz. Tverd. Tela (St. Petersburg) **34**, 743 (1992) [Sov. Phys. Solid State **34**, 398 (1992)].
22. I. I. Antonova, N. M. Nizamutdinov, R. Yu. Abdulsabirov, *et al.*, Appl. Magn. Reson. **13**, 597 (1997).

Translated by O. Borovik-Romanova

View publication stats